Chapter

Structure, Microstructure, and Some Selected Mechanical Properties of Ti-Ni Alloys

Daniela Cascadan and Carlos Roberto Grandini

Abstract

Titanium nickel (Ti-Ni) alloys with low nickel (Ni) content can be used as biomaterials because they improve the mechanical properties, corrosion, and wear resistance of commercially pure titanium (Cp-Ti). Among the mechanical properties of a biomaterial, elastic modulus and microhardness are very important, and each varies according to the microstructure and interstitial elements such as oxygen and nitrogen as well as the amount of substitutional element and thermomechanical processing. Heat treatments are used to obtain a homogeneous microstructure, free of internal stresses structural, microstructural, also to retain or change the size of the phases. In this chapter, the preparation, chemical, structural, and microstructural, and mechanical characterization of Ti-Ni alloys are presented. The structural and microstructural characterization showed the predominant presence of α and Ti_2Ni phases. There is no clear variation of the microhardness due to the amount of nickel. The dynamic elastic modulus was slightly above the Cp-Ti due to the addition of a new intermetallic phase (Ti_2Ni) but did not vary significantly with the amount of Ni.

Keywords: Ti-Ni alloys, structure, microstructure, mechanical properties

1. Introduction

The development of biomaterials has created several significant benefits for the general population over the last few decades, including dental implants, prosthetics, artificial arteries, and contact lenses [1]. These benefits have been either for the purpose of correcting problems or have been esthetic in nature [2].

Various materials have been used as biomaterials. Titanium alloys [3, 4] are among these materials because they have excellent mechanical strength/density ratio, excellent corrosion resistance, and biocompatibility.

The mechanical properties [5], corrosion, and wear resistance [6] of a material are largely dictated by the microstructure. Titanium alloys are favorable because a wide spectrum of microstructures can be obtained, depending on the chemical composition and the processing. This makes titanium alloys advantageous because they allow the desired microstructure to be obtained for specific requirements, as low elastic modulus, for example, [7, 8].

Titanium exists in two allotropic forms. At low temperatures, the so-called alpha phase (with hexagonal compact crystalline structure) is presented, and the beta phase (with body-centered cubic crystalline structure) emerges above 883°C. Some

elements called beta stabilizers, such as niobium, molybdenum, iron, vanadium, and nickel, lead to a decrease in beta transus temperature (the transition from alpha to beta phase) when added to the forming titanium alloys and may stabilize this phase at room temperature. These phases determine a classification of titanium alloys: alloys containing only α stabilizers at this phase are known as α alloys, alloys containing 1–2% beta stabilizers and about 5–10% of beta phase are called near-α, alloys containing increased amounts of beta stabilizers resulting in 10–30% of beta phase are called α + β alloys, and alloys containing increased amounts of beta stabilizers where this phase can be retained by quick cooling are known as β metastable phases (these alloys decay into α + β in aging treatments) [9]. Beta transus temperature fulfills a central role in the microstructure's evolution, and so it is of great importance to determine the type of technological processing and heat treatment, which also includes doping with oxygen or nitrogen, whose elements present in the crystalline lattice can significantly affect the properties of the same [10].

In addition to interfering significantly in the structure and microstructure of titanium alloys, substitutional elements interfere in mechanical properties such as elastic modulus and hardness to the extent that they stabilize phases with different properties [11, 12]. The α phase, with a greater packaging factor of atoms, has a greater elastic modulus in relation to phase β, due to greater proximity between the atoms. Regarding toughness, it is usually greater in α phase, which contains fewer plans of slipping in relation to β phase, making the material harder and brittle [13]. However, depending on the alloy and the processing performed, alloys with a β structure have similar hardness [14].

The presence of atoms in interstitial positions of the lattice (e.g., nitrogen and oxygen) strongly influences some properties, such as mechanical resistance and ductility [15]. These elements act as stabilizers in titanium's α and α' phases, increasing the temperature of β-transus [16, 17].

Nickel causes several adverse reactions in the human body, such as carcinogenic, genotoxic, mutagenic, cytotoxic, and allergenic effects [18]. However, when nickel is connected to titanium, these problems are minimized [19]. In a study of corrosion of titanium alloys with varied concentrations of nickel in Ringer's solution, it was found that the potential of disruption occurs from 29 wt% of nickel and decreases rapidly, indicating that alloys below this concentration present promising applications regarding corrosion [20, 21]. A later study on Hank's biocorrosion solution concluded that the daily release of nickel would be hundreds of times smaller than that contained in water intake [22]. In addition, the microhardness of these alloys is similar to enamel (310–390 HVN), which is suitable for use in dental screws [18].

Thus, it is of fundamental importance to understand the role of substitutional nickel in the structure, microstructure, and selected mechanical properties in Ti-Ni system alloys. To this purpose, Ti-Ni alloys containing 5, 10, 15, and 20 wt% of nickel were melted in an arc-melting furnace, mechanically processed by hot rolling, and subjected to heat treatment in a vacuum to cause homogenization and stress relief.

2. Materials and methods

2.1 Ti-Ni alloys

The phase diagram of the Ti-Ni system is presented in **Figure 1**. This phase diagram shows that alloys considered in this chapter (5, 10, 15, and 20 wt% of nickel) present the phases α and β (both of titanium) and the intermetallic phase Ti_2Ni, at high temperatures [23]. By the lever rule, the higher the nickel

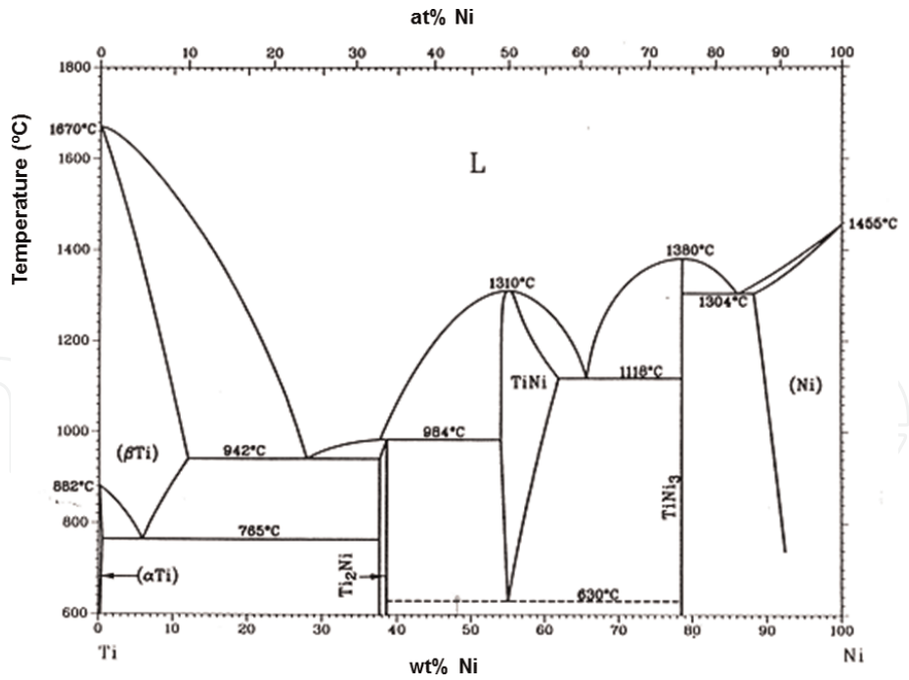

Figure 1.
Phase diagram of the Ti-Ni system [23].

concentration is, the greater the amount of this intermetallic is. By the decay of the β-transus curve, it is concluded that the addition of nickel favors the stabilization of this phase. The eutectoid reaction $\beta \rightarrow \alpha + Ti_2Ni$ occurs at 765°C. By the lever rule, in the field $\beta + Ti_2Ni$, the amount of Ti_2Ni is lower in relation to $\alpha + Ti_2Ni$ field, in the same concentration.

For example, for an alloy with 10 wt% nickel that underwent a homogenization heat treatment at 1000°C, followed by slow cooling, in equilibrium conditions, at this temperature, the alloy presents the β phase of titanium. With cooling, it begins to precipitate the intermetallic phase Ti_2Ni. At a temperature just above 765°C, the precipitates of Ti_2Ni proeutectoid phase are found in a β matrix of eutectoid composition and just below 765°C and are found in the eutectoid matrix, with a granular microstructure of α and Ti_2Ni phases intercalated. From there, the intermetallic Ti_2Ni composes both precipitates and the eutectoid matrix.

Theoretically, the phases present in these alloys at room temperature are $\alpha + Ti_2Ni$; however, when the eutectoid reaction is suppressed, as in the case where the cooling is not done in perfect equilibrium condition, there is the possibility of β-phase retention at room temperature, the higher the nickel concentration is [24].

According to Ti-Ni binary diagram, a eutectic $L \rightarrow \beta + Ti_2Ni$ to 942°C occurs at a concentration of 28.4 wt% of nickel, <700°C in relation to the melting point of pure titanium (1670°C), thus decreasing the melting point and conforming temperature. Therefore, in the case of alloys with 15 and 20 wt% of nickel, at some point during the melting, there is the possibility of developing a microstructure composed of pre-eutectic precipitates of the β phase in a eutectic matrix, although the melting is not done under equilibrium conditions.

The Ti-Ni alloys were prepared using commercially pure titanium (Cp-Ti) (99.7% purity, Aldrich Inc., USA) and nickel (99.5% purity, Camacam Industrial, Brazil). The ingots were obtained by arc melting, using a water-cooled copper crucible and an argon-inert atmosphere. The melting was held five times to ensure the homogeneity of the produced ingots. Samples were prepared with 5, 10, 15, and 20 wt% of nickel. Chemical analysis of the samples was performed using an inductively coupled plasma optical emission spectrometry (ICP-OES), Varian, Visa

model, from the sample's dissolution in acid medium. The presence of interstitial elements was carried out using a LECO TC-400 model gas analyzer. **Table 1** shows the chemical analysis of the produced samples.

It can be verified that the obtained ingots show the correct stoichiometry of nickel and a low amount of impurities and interstitial elements, displaying the good quality of prepared alloys.

To check the homogeneity of the produced alloys, the samples were subjected to a mapping of the elements that comprise the alloys using an electron dispersion spectrometry (EDS) technique that used an Oxford Instruments Incax-act model detector coupled to the scanning electron microscope (SEM) Carl Zeiss EVO/LS15 model. **Figure 2** shows the mapping of the elements titanium and nickel obtained by EDS in the produced alloys after melting. In all cases, homogeneous distribution of the elements titanium and nickel can be observed, showing that the melting was complete, without the presence of aggregates or segregates.

After melting, the ingots were submitted to a homogenization heat treatment that consisted of slowly heating the samples up to 1173 K for 24 h in a vacuum of 10^{-6} Torr, followed by slow cooling in the furnace. The mechanical processing of

Alloy	Fe (wt%)	Al (wt%)	Ni (wt%)	Mn (wt%)	Cr (wt%)	Cu (wt%)	C (wt%)	O (wt%)	N (wt%)
Ti-5Ni	0.07	0.005	5.36	0.020	0.008	0.001	0.124	0.109	0.012
Ti-10Ni	0.10	0.018	10.03	0.034	<0.001	<0.001	0.380	0.179	0.007
Ti-15Ni	0.12	0.035	15.83	0.052	<0.001	<0.001	0.023	0.290	0.058
Ti-20Ni	0.12	0.028	19.80	0.072	<0.001	<0.001	0.160	0.300	0.076

Table 1.
Chemical analysis of the Ti-Ni alloys.

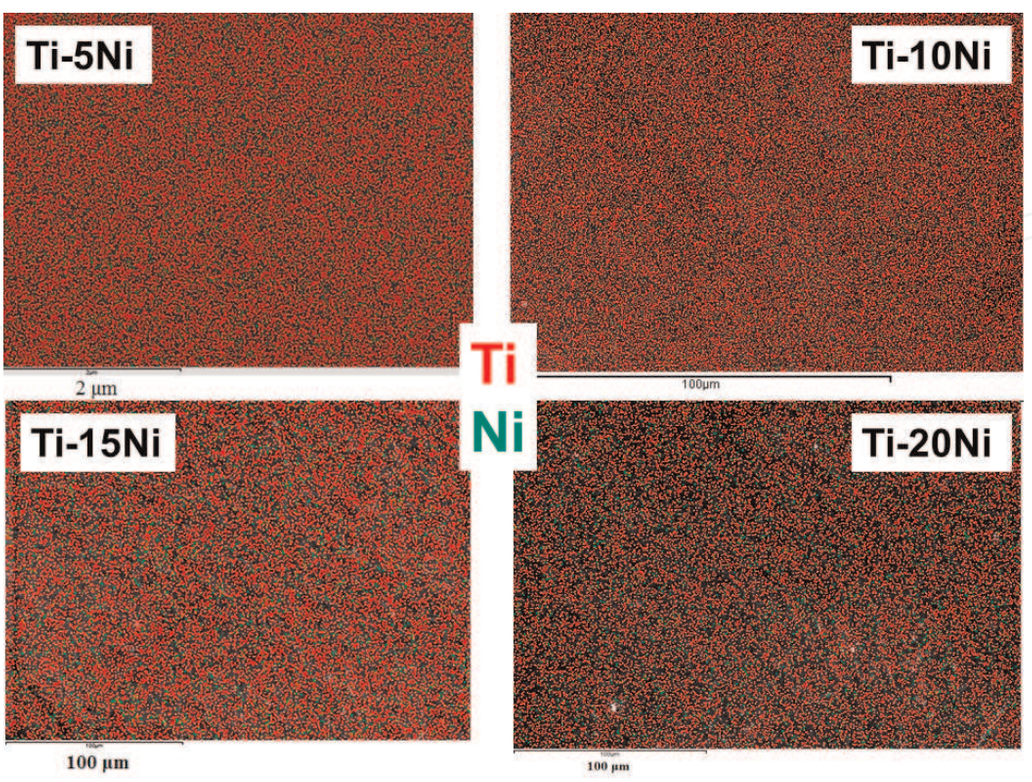

Figure 2.
EDS mapping of the elements Ti and Ni that make up the Ti-Ni alloys.

the samples is important because it allows tests that require symmetrical samples, in addition to causing changes in microstructure and some properties that are of interest in the analysis. The samples were hot rolled as their mechanical processing.

After slow cooling, a new heat treatment was performed for strain relief and recrystallization of microstructures as there were internal stresses and deformed microstructures due to an aggressive hot-rolling process. This treatment was performed at 1143 K for 24 h in a vacuum.

2.2 Sample's characterization

The structural characterization of the samples was carried out by X-ray diffraction (XRD) measurements on a Rigaku diffractometer (D/Max-2100PC model). This included a Cu-Kα radiation of wavelength of 1.544 Å, 20 mA current, and a potential of 40 kV. The fixed mode, with step of 0.02° and time of 1.6 s, in the range of 10–90°, was used. The used method to data acquisition was the powder method [25].

For all samples of the Ti-Ni alloys used in this chapter and in all processing conditions, the microstructure was evaluated by both optical and scanning electron microscopy. To obtain the images, an Olympus model BX51M optical microscope with a camera connected to a computer and a SEM Carl Zeiss EVO/LS15 model with the SmartSEM software were used.

Vickers microhardness tests were performed using a Shimadzu HMV model-2 microdurometer connected to a computer. The load used was 1.941 N for a time of 60 s. Following ASTM standards, almost 20 indentations were made in different regions of the sample [26, 27]. The dynamic elastic modulus was measured using Sonelastic® equipment (ATCP, Brazil). A boost in sample, the frequencies of vibration (through the Sonelastic® software), and damping were calculated and linked with the modulus of elasticity, according to standard ASTM E1876-01 [28].

3. Results and discussion

3.1 Structural characterization

Figure 3 shows the X-ray diffractograms of all samples of Ti-Ni alloys after melting. During analysis of the X-ray diffractograms of samples after melting, it was observed that the addition of at least 10% in the weight of nickel caused the appearance of other phases beyond the α phase of titanium. There is the emergence of intermetallic Ti_2Ni or Ti_4Ni_2O phases (which have the same diffraction pattern) [29, 30], and perhaps a small amount of β phase because nickel is a β-stabilizer element. It was also observed that the higher the amount of nickel was, the greater the amount of intermetallic Ti_2Ni observed in the increased intensity of the peaks and according to the system's phase diagram [23].

Cascadan et al. studied casting Ti-5Ni (wt%) [31] and Ti-10Ni (wt%) [17] concerning structural and microstructural characterization. In the case of Ti-5Ni alloy, in the XRD measurements, single α and α'phases were observed, which were corroborated by optical micrographs, showing Widmanstatten-type morphology in the samples that were subjected to quick cooling from above β transus temperature, while larger lamellar structures were observed in samples whose slow-cooling process allowed large-scale diffusion processes. In the case of Ti-10Ni alloy, the structure and microstructure of the produced alloy were analyzed by XRD and SEM, and the results showed that the alloy presents predominantly titanium α phase, with proeutectoid lamellar precipitates in eutectoid matrix of α phase and intermetallic Ti_2Ni.

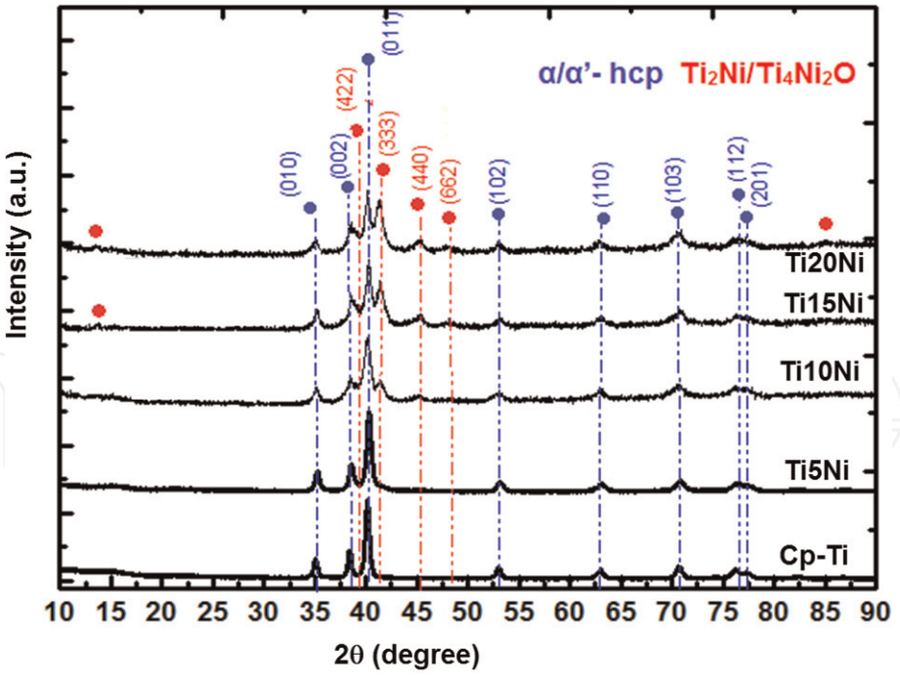

Figure 3.
X-ray diffraction for the Ti-Ni alloys after melting.

Lin et al. produced a Ti-18Ni (wt%) alloy by arc melting and showed the same phases in relation to this paper [32]. However, Ti-Ni alloys produced from metal powders melted with a 5 kW CO_2 laser presented the β phase, in addition to the α and Ti_2Ni phases, which showed that arc melting is a process of higher thermodynamic equilibrium in relation to the laser melting. The same features were observed in the case of Ti-Ni alloys that were quickly solidified for the analysis of metastable microstructures. The metastable microstructure non-equilibrium conditions also allowed the β beyond the expected α and Ti_2Ni phases [33]. In another type of processing, Ti-7Ni alloy samples were produced by sintering at 1200°C for 2 h with heating and cooling rates of 4°C/min. In this case, the peaks of X-ray diffraction of α and Ti_2Ni phases were also observed due to the low cooling rate [34]. The same occurred with the Ti-3Ni sintered to 1300°C for 2 h and heated and cooled at 4°C/min rate, with measurements of X-ray diffraction to 960°C [35]. However, samples of Ti-2Ni and Ti-5Ni sintered at 800 and 1100°C for 1 h with a heating rate of 10°C/min and cooled in the furnace presented α phase, in addition to the intermetallic Ti_2Ni and $TiNi_3$ phases. In this paper, it was found that the higher the sintering temperature and the amount of Ni are, there were higher quantities of intermetallic phases due to the diffusion process that allowed the reaction between Ti and Ni elements [36].

Peak shifts were also observed, which indicated changes in the lattice and angle parameters as well as differences in their format. The asymmetry of the lattice and angle parameters signaled distortion in the crystalline lattice because of the different quantities of substitutional and interstitial elements [15]. The α phase peaks shifted to smaller angles with the increased amount of nickel. This type of displacement is related to the increase in the lattice parameter [25] because the nickel has an atomic radius of 0.078 nm, slightly higher compared to that of titanium (0.076 nm). However, the substitutional element was not the only factor that influenced the lattice parameter; the interstitial elements and mechanical processing can also influence it [37]. In the case of the range of intermetallic phases' peaks, although the elements titanium and nickel were constant, there was a displacement of the peaks due to the presence of nitrogen and oxygen in interstitial positions.

3.2 Microstructural characterization

Figure 4 shows the optical micrographs, and **Figure 5** shows the scanning electron microscopy micrographs of all samples of Ti-Ni alloys, after melting.

For the sample with 5 wt% Ni, according to the phase diagram (**Figure 1**), there must be a certain amount of Ti_2Ni intermetallic phase, whose peak was not observed in the X-ray diffractogram because it was such a small portion, and it was not displayed by optical microscopy either due to the equipment's resolution.

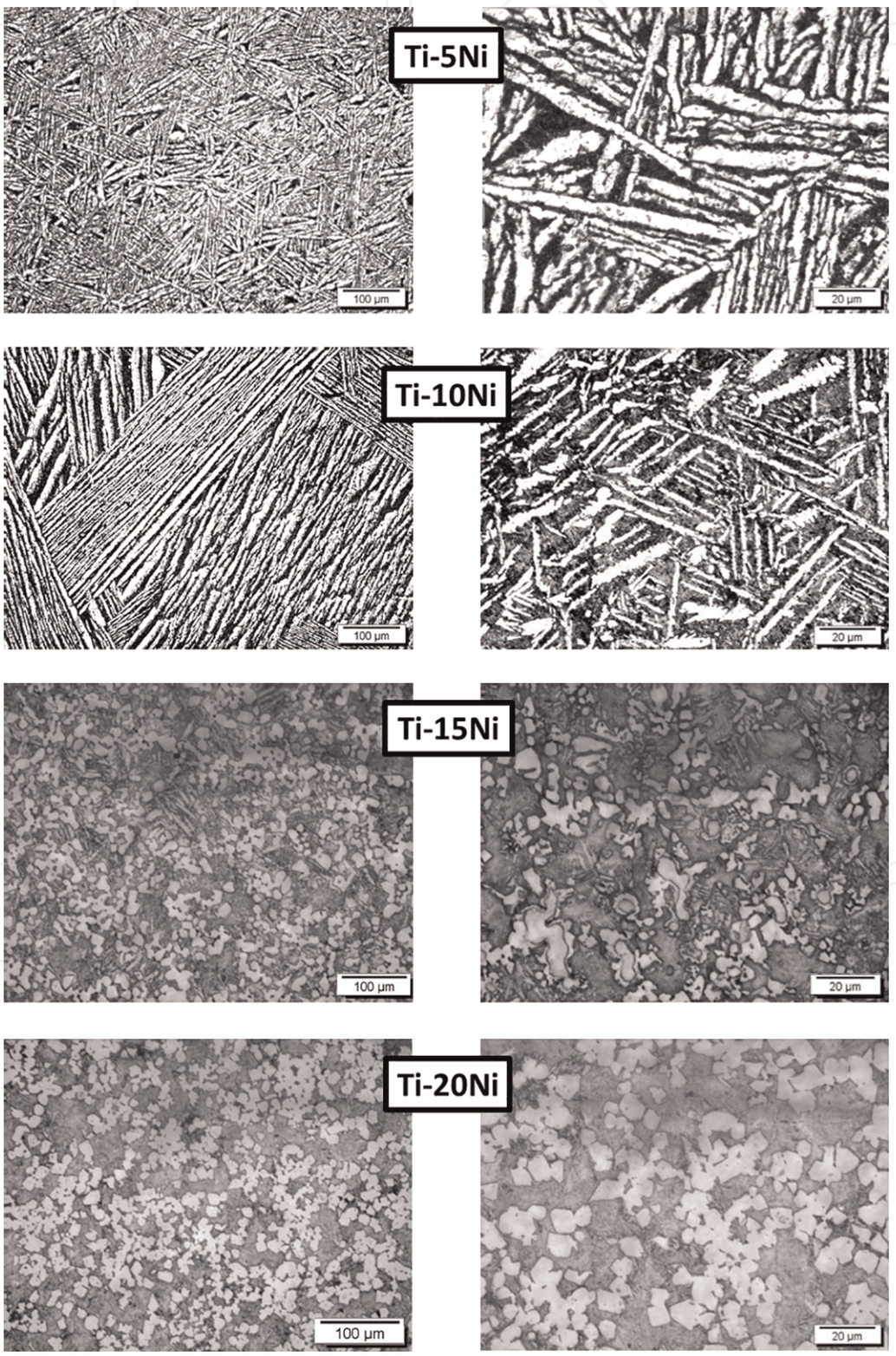

Figure 4.
Optical micrographs for Ti-Ni alloys after melting.

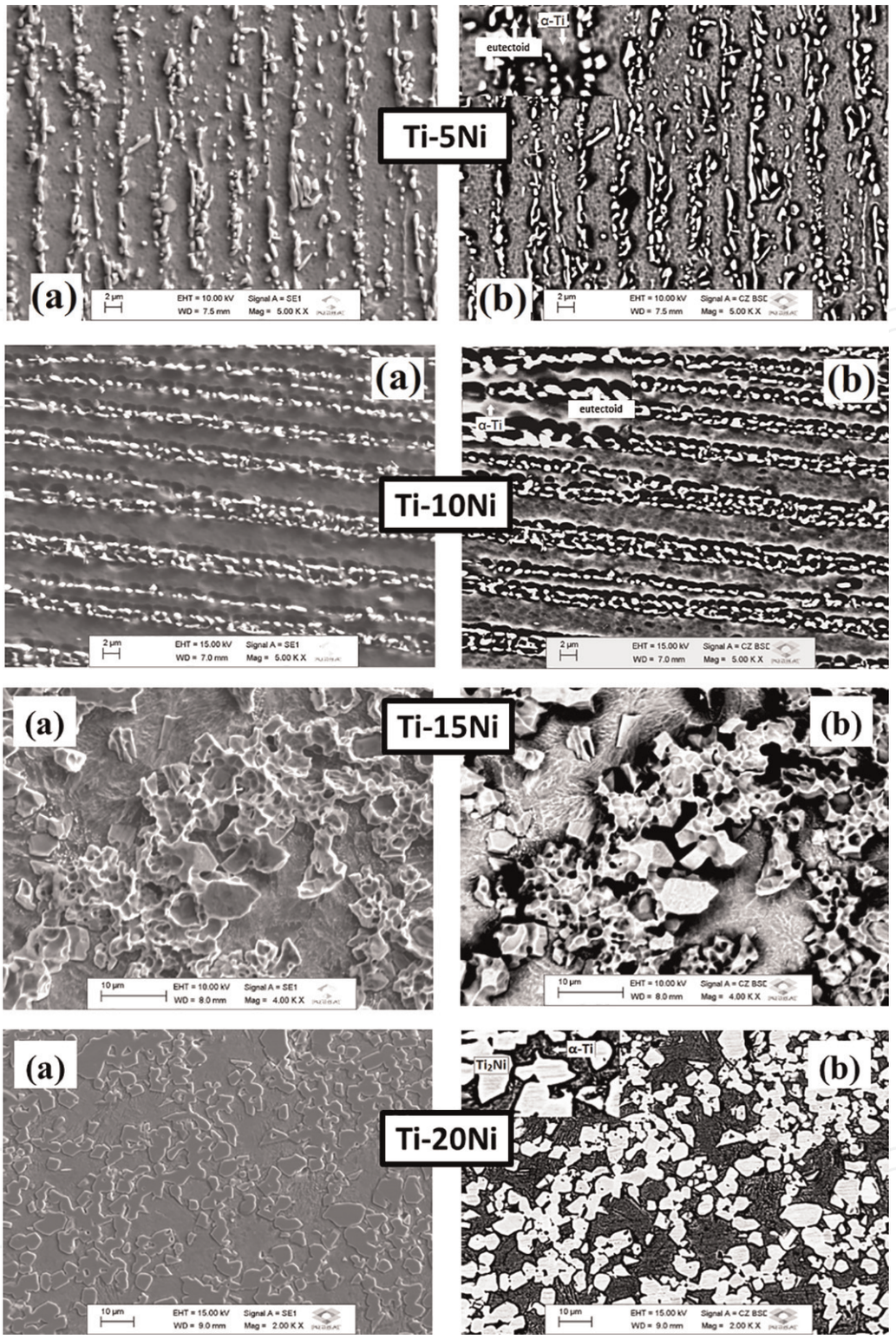

Figure 5.
SEM micrographs for the Ti-Ni alloys after melting, (a) secondary and (b) backscattering electrons.

However, the dark regions between the lamellae of the α phase clearly were a eutectoid microstructure characterized by two phases, alternating between α and Ti_2Ni itself. This eutectoid microstructure was like the microstructure of the sintered Ti-3Ni alloy shown in small expansion, but a larger magnification electron microscopy clearly showed this eutectoid microstructure [35]. In the SEM micrographs (**Figure 5**), between the lamellae of the α phase, the presence of a eutectoid microstructure characterized by two phases was observed, alternating between α

and Ti_2Ni. This microstructure was considered hypoeutectoid because the concentration of 5 wt% of nickel was slightly lower than the concentration of about 6%, where the eutectoid reaction occurs [31]. The presence of the intermetallic phase that contained higher concentrations of nickel was evident in the micrographs for backscattered electrons, where the lighter area comprised the region with the highest average atomic number and the nickel had a higher atomic number compared to titanium.

For the alloy with 10 wt% of nickel, observed by optical micrographs (**Figure 4**), the microstructure consisted of precipitates of titanium proeutectoid α phase (clear) in a matrix of eutectoid microstructure (dark region) comprised of alternating lamellae of α and Ti_2Ni phases, also known as pearlite [38]. According to the phase diagram (**Figure 1**), the eutectoid reaction occurred at a nickel concentration of 6 wt%, and thus the alloy presented hypereutectoid composition, and the precipitates would be Ti_2Ni or Ti_4Ni_2O, in view of the small amount of nickel. Furthermore, α phase precipitates characterize an alloy of hypoeutectoid composition. The high quantities of oxygen and nitrogen (stabilizers of α phase) can cause change in the composition of this reaction [39]. The increase of the concentration of nickel, from the composition of about 6 wt%, does not act as a β-phase stabilizer, but causes an increase in the temperature of the formation of intermetallic phase Ti_2Ni. The images obtained by SEM (**Figure 5**) allowed more details to be obtained. At the junction of three lines where grain and leaving these needles of the α phase microstructure perpendicular to each other did originate in the grain boundaries when phase change occurred. This microstructure is similar to a Ti-24Al-11Nb alloy, whose intermetallic phase Ti_3Al locates on the grain boundaries and metallic matrix [39]. Also, according to Liu et al. [29], the diffusion of oxygen in grain boundaries is higher than in its interior, and the precipitates of Ti_4Ni_2O are formed over these. Such morphology is proven by the images obtained by backscattering electrons, where lighter points indicate the intermetallic phase between the lamellae of the α phase.

Unlike the Ti10Ni samples in the initial conditions of processing, in samples of Ti15Ni, a proeutectoid of Ti_2Ni presents precipitates which probably reacted with oxygen, thus forming Ti_4Ni_2O, comparing the amount of nickel and precipitates. This microstructure is similar to that shown by Chern lin et al. [20] and was expected due to the higher concentration of nickel in a matrix with the α phase in accordance with the X-ray diffractograms for this sample and the system's phase diagram. The optical micrographs show lighter regions that are proeutectoid of Ti_4Ni_2O precipitates in α + Ti_2Ni array. The same morphology was observed in micrographs obtained by a SEM, both for secondary electrons as backscattered, shown in **Figure 5**. Dendritic structures were also obtained by Xu et al. in Ti with 20 wt% Ni alloy procured by laser melting [24].

3.3 Mechanical characterization

Figure 6 shows the values of microhardness and elastic modulus according to the amount of nickel in the homogenized condition after hot rolling. Due to experimental conditions, the microhardness and elastic modulus measurements were made only after homogenized condition after hot-rolling conditions. There is no relationship between these properties because they involve different processes: microhardness is a measure of resistance to a plastic deformation; and elastic modulus depends on the binding force between the atoms. A factor that increases microhardness is the increase in the concentration of the substitutional element because atoms of different sizes in the crystalline lattice cause deformation in it, creating obstacles to the movement of dislocations [13]. There is also no direct

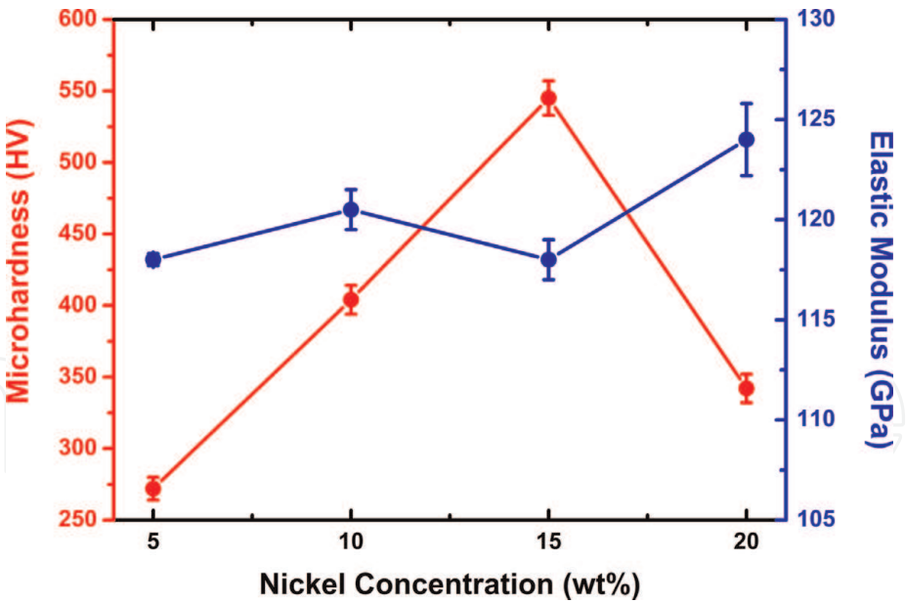

Figure 6.
Microhardness and elastic modulus values for Ti-Ni alloy samples in homogenized condition, after hot rolling.

relationship between such quantities and the amount of nickel because this is not the only factor involved.

A large variation in microhardness values was observed from 250 to 590 HV. Several factors influence a material's hardness: the concentration of substitutional and interstitial elements, microstructure, size of grain boundaries, types of phases, crystallographic orientation in which deformation occurs (since it involves a plastic deformation), and the type of processing [13]. The Ti-Ni alloy samples used in this chapter presented considerable variations of these factors.

To analyze whether these values were in agreement with those found in the literature, it was used specifically by Chern Lin et al., with similar preparation of Ti-Ni alloys by arc melting and nickel concentration ranging from 18 to 28.4 wt%. The authors obtained microhardness values ranging from 300 to 390 HV [20]. In the present study, the microhardness ranged from 345 to 390 HV, values aligned approximately with Lin's study. For Ti-Ni alloys with nickel concentration varying from 10 to 20 wt% obtained by laser fusion of metal powders [32], the microhardness ranged from 270 to 510 HV due to the increase of Ti_2Ni precipitates. Although the phases are different in relation to this study and other metallic atoms are present, the values are approximate with Lin's in relation to the other conditions, although the experimental parameters are not explicit in both cited studies.

For the Ti15Ni alloy, a high value for the microhardness was observed. As mentioned earlier, the increase of the concentration of nickel, from the composition of about 6 wt%, does not act as a β-phase stabilizer but causes an increase in the temperature of the formation of intermetallic phase Ti_2Ni that can be responsible for this increase in the hardness value [21]. In samples of Ti15Ni, a proeutectoid of Ti_2Ni presents precipitates which probably reacted with oxygen, thus forming Ti_4Ni_2O, comparing the amount of nickel and precipitates. The formation of Ti_4Ni_2O phase is another component to increase the hardness of the Ti15Ni alloy [15, 21].

The elastic modulus for Cp-Ti is around 95–105 GPa [9]. Thus, the addition of nickel caused a small increase in this property, probably from the addition of a new fcc phase referring to intermetallic Ti_2Ni. However, as shown in **Figure 6**, it was not observed as a proportional ratio of the elastic modulus with the nickel concentration.

4. Summary

The Ti-Ni samples obtained by arc melting were adequately prepared regarding stoichiometry and homogeneity and characterized by XRD, SEM, and selected mechanical properties.

The alloys showed the presence of α, Ti_2Ni, and Ti_2Ni_4O, due to the reaction of the intermetallic Ti_2Ni with oxygen. The microhardness results showed values in accordance with those presented in the literature, suitable for the use of fixation devices. There is no clear variation of the microhardness due to the amount of nickel because there were several factors involved, and the microstructures were very diversified and complex. The dynamic elastic modulus was slightly above the Cp-Ti due to the addition of a new intermetallic phase but did not vary significantly with the amount of nickel.

Acknowledgements

The authors would like to acknowledge the Brazilian agencies Capes, for D. Cascadan's fellowship, CNPq (grants #481313/2012-5 and #307.279/2013-8), and FAPESP (grant #2015/25.562-7) for their financial support.

Author details

Daniela Cascadan[1,2] and Carlos Roberto Grandini[1,2]*

1 Laboratório de Anelasticidade e Biomateriais, UNESP—Univ. Estadual Paulista, Bauru, SP, Brazil

2 IBTN/Br—Institute of Biomaterials, Tribocorrosion and Nanomedicine-Brazilian Branch, Bauru, SP, Brazil

*Address all correspondence to: carlos.r.grandini@unesp.br

References

[1] Zadpoor AA. Biomaterials and tissue biomechanics: A match made in heaven? Materials. 2017;**10**(5):528

[2] Williams D. The relationship between biomaterials and nanotechnology. Biomaterials. 2008; **29**(12):1737-1738

[3] Kolli R, Devaraj A. A review of metastable beta titanium alloys. Metals. 2018;**8**(7):506

[4] Li Y, Yang C, Zhao H, Qu S, Li X, Li Y. New developments of Ti-based alloys for biomedical applications. Materials. 2014;**7**(3):1709-1800

[5] Li Z, Zhao S, Ritchie RO, Meyers MA. Mechanical properties of high-entropy alloys with emphasis on face-centered cubic alloys. Progress in Materials Science. 2019;**102**:296-345

[6] Manam NS, Harun WSW, Shri DNA, Ghani SAC, Kurniawan T, Ismail MH, et al. Study of corrosion in biocompatible metals for implants: A review. Journal of Alloys and Compounds. 2017;**701**:698-715

[7] Geetha M, Singh AK, Asokamani R, Gogia AK. Ti based biomaterials, the ultimate choice for orthopaedic implants—A review. Progress in Materials Science. 2009;**54**(3):397-425

[8] Nasab MB, Hassan MR. Metallic biomaterials of knee and hip—A review. Trends in Biomaterials and Artificial Organs. 2010;**24**(1):69-82

[9] Leyens C, Peters M. Titanium and Titanium Alloys: Fundamentals and Applications. New York: Wiley-VCH; 2005

[10] Boureau G, Capron N, Tétot R. A first-principles study of dilute solutions of oxygen in titanium. Scripta Materialia. 2008;**59**(12):1255-1258

[11] Silva LMD, Claro APRA, Buzalaf MAR, Grandini CR. Influence of the substitutional solute on the mechanical properties of Ti-Nb binary alloys for biomedical use. Materials Research. 2012;**15**:355-358

[12] Noumbissi S, Scarano A, Gupta S. A literature review study on atomic ions dissolution of titanium and its alloys in implant dentistry. Materials. 2019;**12**(3): 368

[13] Callister W. Materials Science and Engineering: An Introduction. New Jersey: John Wiley & Sons; 2007

[14] Manda P, Chakkingal U, Singh AK. Hardness characteristic and shear band formation in metastable β-titanium alloys. Materials Characterization. 2014; **96**:151-157

[15] Fast JD. Gases in Metals. London: Macmillan; 1976

[16] Min X, Bai P, Emura S, Ji X, Cheng C, Jiang B, et al. Effect of oxygen content on deformation mode and corrosion behavior in β-type Ti-Mo alloy. Materials Science and Engineering A. 2017;**684**:534-541

[17] Cascadan D, Grandini CR. Influence of thermo-mechanical treatments on the structure and microstructure of alloy of titanium Ti-10%pNI obtained by arch fusion. Matéria. 2015;**20**(2): 368-373

[18] Biesiekierski A, Wang J, Abdel-Hady Gepreel M, Wen C. A new look at biomedical Ti-based shape memory alloys. Acta Biomaterialia. 2012;**8**(5): 1661-1669

[19] Sevcikova J, Pavkova Goldbergova M. Biocompatibility of NiTi alloys in the cell behaviour. Biometals. 2017;**30**(2): 163-169

[20] Chern Lin JH, Lo SJ, Ju CP. Biocorrosion study of titanium-nickel alloys. Journal of Oral Rehabilitation. 1996;**23**(2):129-134

[21] Chern Lin J-H, Moser JB, Taira M, Greener EH. Cu-Ti, Co-Ti and Ni-Ti systems: Corrosion and microhardness. Journal of Oral Rehabilitation. 1990; **17**(4):383-393

[22] Dinca VC, Soare S, Barbalat A, Dinu CZ, Moldovan A, Stoica I, et al. Nickel-titanium alloy: Cytotoxicity evaluation on microorganism culture. Applied Surface Science. 2006;**252**(13): 4619-4624

[23] Otsuka K, Ren X. Martensitic transformations in nonferrous shape memory alloys. Materials Science and Engineering A. 1999;**273-275**:89-105

[24] Lin X, Chen J, Huang W. Microstructure evolution of Ti-20wt% Ni alloy in laser solid forming. Acta Metallurgica. 2008;**44**(8):1013-1018

[25] Cullity BD, Stock SR. Elements of X-Ray Diffraction. 3rd ed. New York: Prentice Hall; 2001

[26] ASTM E384-11. Standard Test Method for Knoop and Vickers Hardness of Materials. Vol. ASTM E384-11. West Conshohocken, PA: ASTM International; 2011

[27] ASTM E92-82. Standard Test Method for Vickers Hardness of Metallic Materials. Vol. ASTM E92-82. West Conshohocken, PA: ASTM International; 2003

[28] ASTM E1876-01. Standard Test Method for Dynamic Young's Modulus, Shear Modulus, and Poisson's Ratio by Impulse Excitation of Vibration. Vol. E 1876-01. Philadelphia, USA: ASTM International; 2002

[29] Liu XP, Cao M, Jin W, Meng CG, Yang D. Effect of annealing temperature on transformation behaviors of Ti-50.2 at. pct Ni thin film. Journal of Materials Science and Technology. 2001;**17**(S1): 40-42

[30] ICSD. Inorganic Crystal Structure Database. 2014. Available from: http://icsd.ill.eu/icsd/index.php

[31] Cascadan D, Buzalaf MAR, Grandini CR. Effect of heat treatment on microstructure and mechanical properties of Ti-5wt-%Ni alloys for use as biomaterial. International Heat Treatment and Surface Engineering. 2014;**8**(3):107-110

[32] Lin X, Yue TM, Yang HO, Huang WD. Phase evolution in laser rapid forming of compositionally graded Ti-Ni alloys. Journal of Engineering Materials and Technology. 2009;**131**(4): 041002-041002-5

[33] Nagarajan R, Aoki K, Chattopadhyay K. Microstructural development in rapidly solidified Ti-Ni alloys. Materials Science and Engineering A. 1994;**179–180**(Part 1): 198-204

[34] Luo SD, Yang YF, Schaffer GB, Qian M. The effect of a small addition of boron on the sintering densification, microstructure and mechanical properties of powder metallurgy Ti-7Ni alloy. Journal of Alloys and Compounds. 2013;**555**:339-346

[35] Yang YF, Luo SD, Bettles CJ, Schaffer GB, Qian M. The effect of Si additions on the sintering and sintered microstructure and mechanical properties of Ti-3Ni alloy. Materials Science and Engineering A. 2011; **528**(24):7381-7387

[36] Panigrahi BB. Sintering behaviour of Ti-2Ni and Ti-5Ni elemental powders. Materials Letters. 2007;**61**(1):152-155

[37] Martins JRS Jr, Araújo R, Donato T, Arana-Chavez V, Buzalaf M,

Grandini C. Influence of oxygen content and microstructure on the mechanical properties and biocompatibility of Ti-15 wt%Mo alloy used for biomedical applications. Materials. 2014;**7**(1): 232-243

[38] Diebold TP, Aaronson HI, Franti GW. Influence of interphase boundary structure upon the mechanism of eutectoid decomposition in a Ti-Ni alloy. Metallurgical Transactions A. 1978;**9**(9):1339-1341

[39] Lütjering G, Williams JC. Titanium. 2nd ed. Berlin: Springer; 2007